MEASUREMENT OF TYRE/PAVEMENT INTERFACE STRESSES UNDER MOVING WHEEL LOADS

M de Beer

Reprint of paper accepted for presentation at the Vehicle-Road and Vehicle-Bridge Interaction Conference, June 5 - 10, 1994, Noordwijkerhout, The Netherlands

April 1994 **Research Report DPVT 224**

Roads and Transport Technology

CSIR

DOCUMENT RETRIEVAL INFORMATION

REPORT NO:	DPVT 224	DATE OF ISSUE:	PAGES
ISBN:	0-7988-5443-X	April 1994	20 + (v)

TITLE: Measurement of tyre/pavement interface stresses under moving wheel loads

AUTHOR: M de Beer

Issuing organisation:
Pavement Engineering Technology
Division of Roads and Transport Technology
CSIR, P O Box 395, Pretoria

Keywords: Stress, pavement, tyre, array, load cell, tyre/pavement interface

Sinopsis:

Akkurate ontwerp-inset-parameters is van kritieke belang in die ontwerp van meer ekonomiese padstrukture. Die band/plaveisel kontakvlakspannings is een van die mees belangrike insette in enige plaveiselontwerpsisteem en dit is dus noodsaaklik om dit toepaslik te definieer. Hierdie referaat beskryf 'n prototipe Voertuig-Pad Oppervlak Druk Omsetter (VPODO) wat ontwikkel is vir die meting van band/plaveisel kontakspannings van 'n bewegende rubberbandwiel. Dit word getoon dat band/plaveisel kontakspannings van 'n bewegende wiel voldoende gemeet kan word in die vertikale-, dwars- en langsrigtings van die bewegende band. Aangesien die sisteem wat hier bespreek word bloot eksperimenteel was en dus sekere onakkuraathede bevat, word sekere verbeteringe voorgestel.

Synopsis:

In order to design more economical pavements it is necessary to use the most accurate input parameters possible. Tyre/pavement interface stresses is one of the most important inputs in any pavement design system and therefore requires appropriate definition. This paper describes a prototype Vehicle-Road Surface Pressure Transducer Array (VRSPTA) system developed for the measurement of the tyre/pavement interface stresses of a moving wheel load. It illustrates that the tyre/pavement stresses caused by a moving wheel can be adequately measured in vertical, transverse and longitudinal directions. As this was an experimental system, which contains some inaccuracies, certain improvements to the current system are also suggested in this paper.

LIST OF CONTENTS

LIST OF CONTENTS

PAGE

LIST OF FIGURES

LIST OF TABLES

1. INTRODUCTION

Throughout the world pavement design engineers are faced with the problem of designing economical pavements. In many areas like southern Africa, the cost of asphaltic layers usually dominates the cost of the pavement. It is therefore important to design towards an optimum asphalt layer thickness in relation to the pavement structural capacity situation. One of the key elements in the design process is the expected traffic loadings over the design life of the pavement. The two most important traffic loading components are axle loads and tyre pressures. Most of the widely used pavement design methods are based on the principle of "equivalent loads" where a traffic axle load spectrum is represented by a static single equivalent design load for the pavement (SARB, 1993; Ioannides et al, 1993; Huang, 1993). Likewise, simply stated, a static uniform tyre contact stress distribution is usually assumed to simulate tyre/pavement interface vertical stresses as input towards the design and evaluation of pavements. This approach is usually adequate for relatively thick (> 75 mm) asphaltic surfacing and base layers, but is highly inaccurate for thinner layers. Horizontal tensile strains resulting from non-uniform stress distribution compared to the "uniform" case can be much higher (up to 100 % more) (Tielking et al, 1987).

For thicker asphaltic concrete layers the potential for permanent (plastic) deformation also closely related to actual tyre/pavement contact stresses (Eisenmann et al, 1987). It is therefore of critical importance to ensure the accurate quantification of the actual stresses at the tyre/pavement interface. During the accelerated pavement testing (APT) programme with the fleet of Heavy Vehicle Simulators (HVSs) in South Africa (Freeme et al, 1982a, 1982b), it was decided to design an experimental Vehicle-Road Surface Pressure Transducer Array (VRSPTA) system. The VRSPTA discussed in this paper was developed in association with the Laboratory of Advanced Engineering (Pty) Ltd., Centre for Structural Mechanics, University of Pretoria, South Africa.

This paper describes some development considerations of the VRSPTA prototype system in the light of actual measured tyre/pavement stresses in the vertical, longitudinal and transverse directions of a slow moving wheel under the Heavy Vehicle Simulator (HVS) system. Some pre-liminary results are also discussed.

2. DESIGN OF THE VEHICLE-ROAD SURFACE PRESSURE TRANSDUCER ARRAY (VRSPTA)

3. GENERAL

The Vehicle-Road Surface Pressure Transducer Array (VRSPTA), or load cell, was designed to simultaneously measure vertical, longitudinal and lateral loads and load distributions transferred to the road surface by a passing wheel. The concept is based on instrumented and calibrated pins buried in the surface of the pavement. Similar systems have been used elsewhere (Martin, 1936; Bonse et al, 1959). These loads and load distributions were to be measured over the complete tyre contact area. To achieve this objective an array of strain-gauged load cell pins were installed in a row, at right angles to the direction of travel of the passing wheel. The strain outputs from these strain-gauged pins were scanned at a high rate while the wheel traversed the pins, giving an indication of vertical, longitudinal and lateral loads acting on each pin.

4. LOAD CELL PINS

The design of the load cell pins had to achieve two objectives:

- Maximum sensitivity of the vertical as well as lateral and longitudinal directions and secondly;
- Achievement of sufficient strength in all three directions to prevent any yielding of the pin material. For the accurate measurement of the strains it was furthermore necessary to achieve local stress fields without high stress gradients to render the measurements less sensitive to the positioning of the strain gauges. In order to obtain high strength yet machinable load cell pins, the pins were manufactured from high tensile steel. After machining, the pins were heat treated to achieve a high yield strength and to reduce hysteresis of the material stress-strain curve. The area of the measuring pins is 73,9 mm^2 (0,115 $inch^2$).

5. SURROUNDING STIFFNESS

Since the load induced by the tyre would be transferred to the array of load cell pins, the area around the pins required a stiffness similar to that of the instrumented pins in order not to alter the tyre load distribution. For the prototype VRSPTA discussed here, a matrix of square pins (area 100 mm^2) was machined from a solid block of grade 50 mild steel. These square pins had the same stiffness as the instrumented pins in the lateral and longitudinal directions, but had a higher, vertical stiffness than the instrumented pins. The top area (tyre contact area) of the square pins was also greater than that of the instrumented pins. (A more advanced VRSPTA is currently under testing and evaluation where all the pins are of the same geometry as the instrumented pins).

6. MANUFACTURE AND INSTRUMENTATION OF LOAD CELL

6.1 <u>Square pin matrix</u>

The square pin matrix was made in three sections for ease of manufacture. These three sections were bolted together through a solid base plate.

6.2 Load cell pins

The instrumented pins were manufactured from high tensile steel by numerical control (NC) machining. After machining, the pins were heat treated to increase the yield strength of the material and to reduce hysteresis of the material stress-strain curve.

The following strain gauges were applied to each of the pins:

- For vertical axial loading: Four (4) 1 mm grid length 90° rosettes.
- For horizontal bending loads: Four (4) 2 mm grid length 90° rosettes.

6.3 Instrumentation

Owing to expected wheel passing velocities of up to 80 km/h, it was not possible to use carrier wave signal conditioning bridges. Direct current (DC) signal conditioners were utilized with switches to enable switching between the three measuring direction channels.

7. CALIBRATION OF INDIVIDUAL LOAD CELL PINS

The individual load cell pins were calibrated in a special calibration jig which was able to apply pre-determined loads to each load cell pin. Each pin was calibrated individually by applying the loads in each direction consecutively.

8. MEASUREMENTS UNDER HVS

8.1 Data recording equipment

A frequency modulation (FM) tape recorder was connected to the analogue output of the strain gauge signal conditioners for recording of the data. Micro switches were installed just before and just after the load cell. These switches acted as instrumentation triggers as well as wheel passing velocity sensors. The operation of the micro switches was hence also recorded.

8.2 Measurement procedures

The following conditions were recorded:

- HVS wheel load: 20 kN, 40 kN, 60 kN, 80 kN
- Wheel velocity: 4 km/h, 6 km/h, 8 km/h
- Tyre pressure: 520 kPa, 570 kPa, 620 kPa

A used Goodyear 1100 x 20, 14 ply rating (cross ply) tyre with the tread (15,5 mm) trimmed down (typical before re-treading) to provide a smooth surface was used for the measurements by the VRSPTA system discussed in this paper.

8.3 Results of initial testing and discussion

The test matrix used is summarized in Table 1. Typical results after data evaluation are illustrated in Figures 1 to 15. These figures indicate that the different stress patterns as predicted by theory (Tielking et al, 1987) can be measured for the vertical, transverse and longitudinal directions of a moving tyre under load. Although some inaccuracies exist with the prototype VRSPTA system discussed here, important observations can already be made.

Of the most important observations from the figures are the following:

(i) Measured stress patterns appears to be similar to those predicted by theory (Tielking et al, 1987).

(ii) The stress patterns compare favourably to stresses measured by other researchers (Bonse et al, 1959; Kasahara et al, 1992; Martin, 1936; Tielking et al, 1994; Yap, 1988).

(iii) From Table 1 the following observations regarding the prototype VRSPTA discussed here can also be made.

(a) Direct measured vertical loads underestimate the applied loads by approximately 25 per cent. The amount of scatter (standard error of measured load approximately 4,4 kN) is also unacceptable.

(b) Resultant transverse load for a free rolling (i.e. no shear) wheel is less than 2 per cent of measured (resultant) vertical load. In theory the resultant transverse force of a free rolling wheel should be zero, but owing to the VRSPTA limitation, a wheel which is not perfectly round and uneven surfaces it appears impossible to achieve this ideal condition at this stage.

(c) Resultant transverse load for a non-free rolling wheel (i.e. with shear) appears to increase with increase in vertical load at constant tyre inflation pressure and constant wheel velocity. However, the magnitude of the resultant transverse load is less than 3 per cent of the measured vertical load (within the test constraints used here).

(d) The resultant longitudinal force appears to increase with wheel load and decrease with increase in tyre inflation pressure. The magnitude of the resultant longitudinal force appears also to be less than 3 per cent of the measured vertical load. This resultant longitudinal force measured here can be a good indication of the "rolling resistance" of a moving tyre on a road pavement.

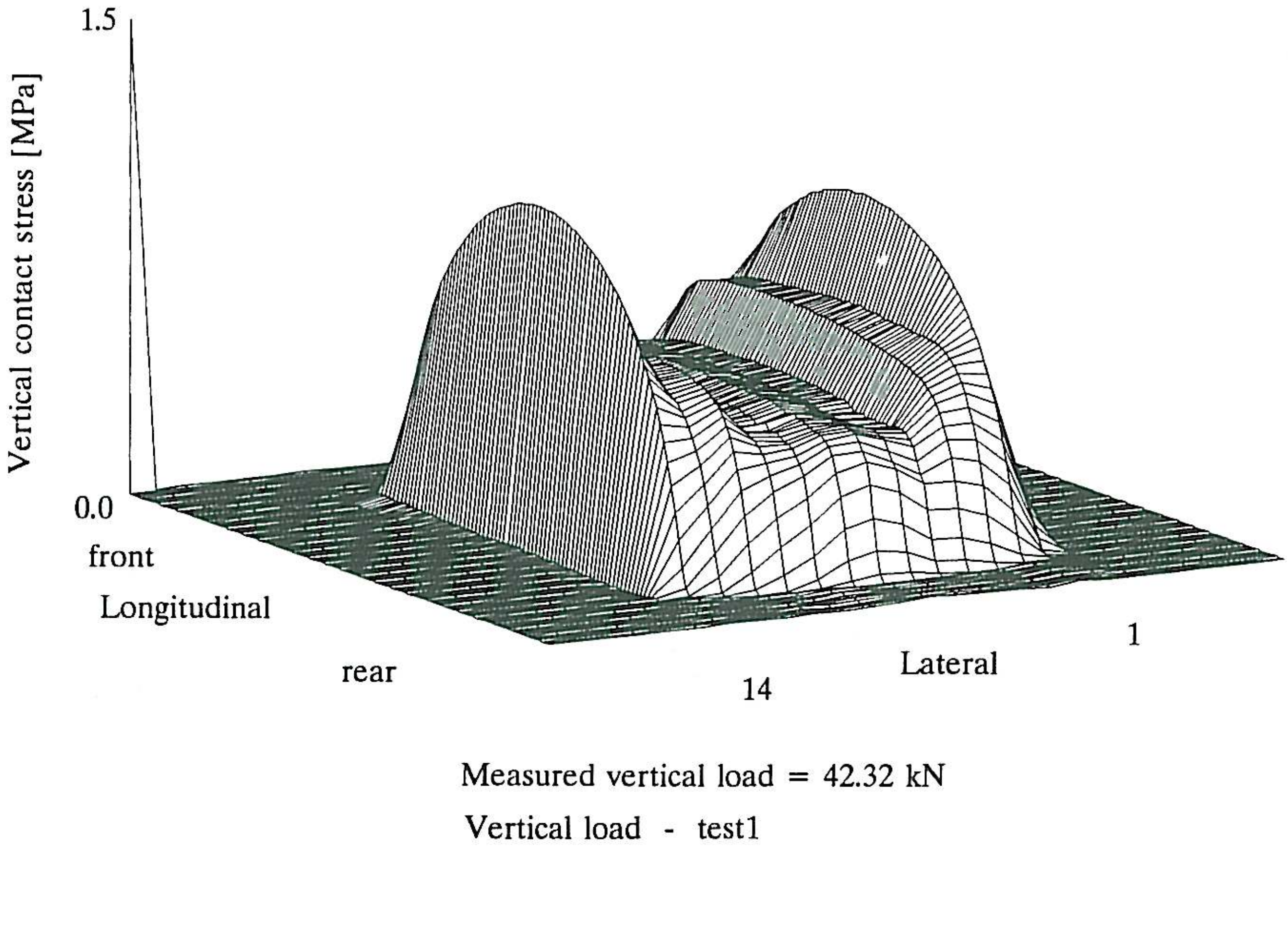

Figure 1: Measured vertical stress distribution of a 60 kN load, tyre inflation pressure 620 kPa and speed of 8 km/h

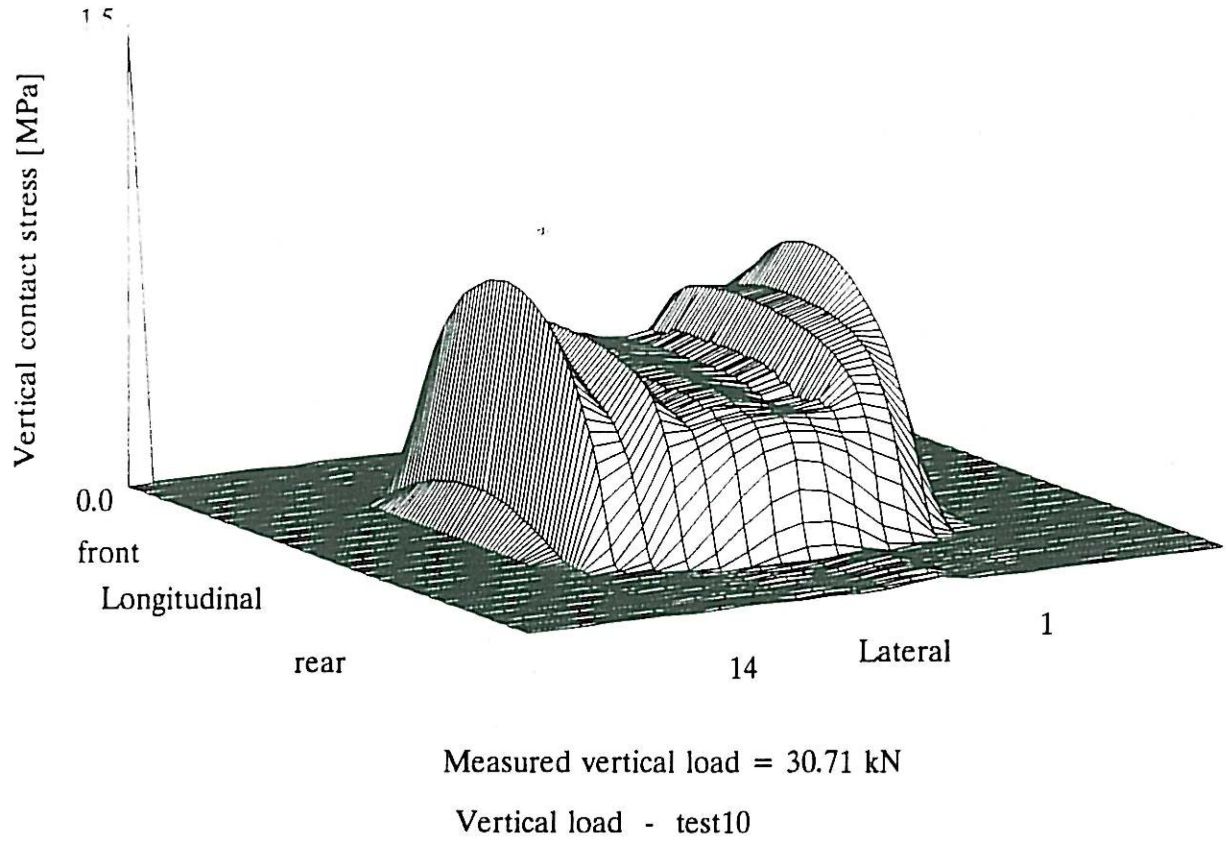

Figure 2: **Measured vertical stress distribution of a 40 kN load, tyre inflation pressure 620 kPa and a speed of 8 km/h**

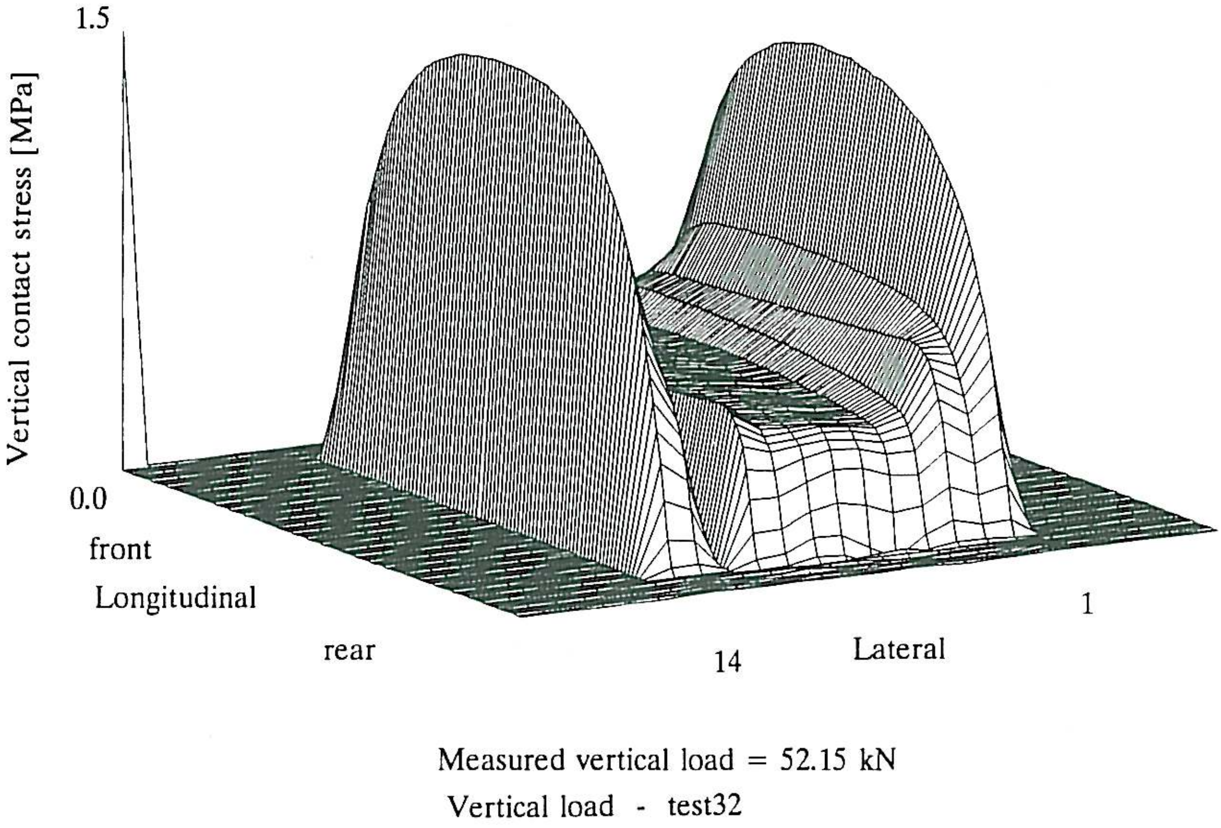

Figure 3: **Measured vertical stress distribution of a 80 kN load, tyre inflation pressure 620 kPa and a speed of 8 km/h**

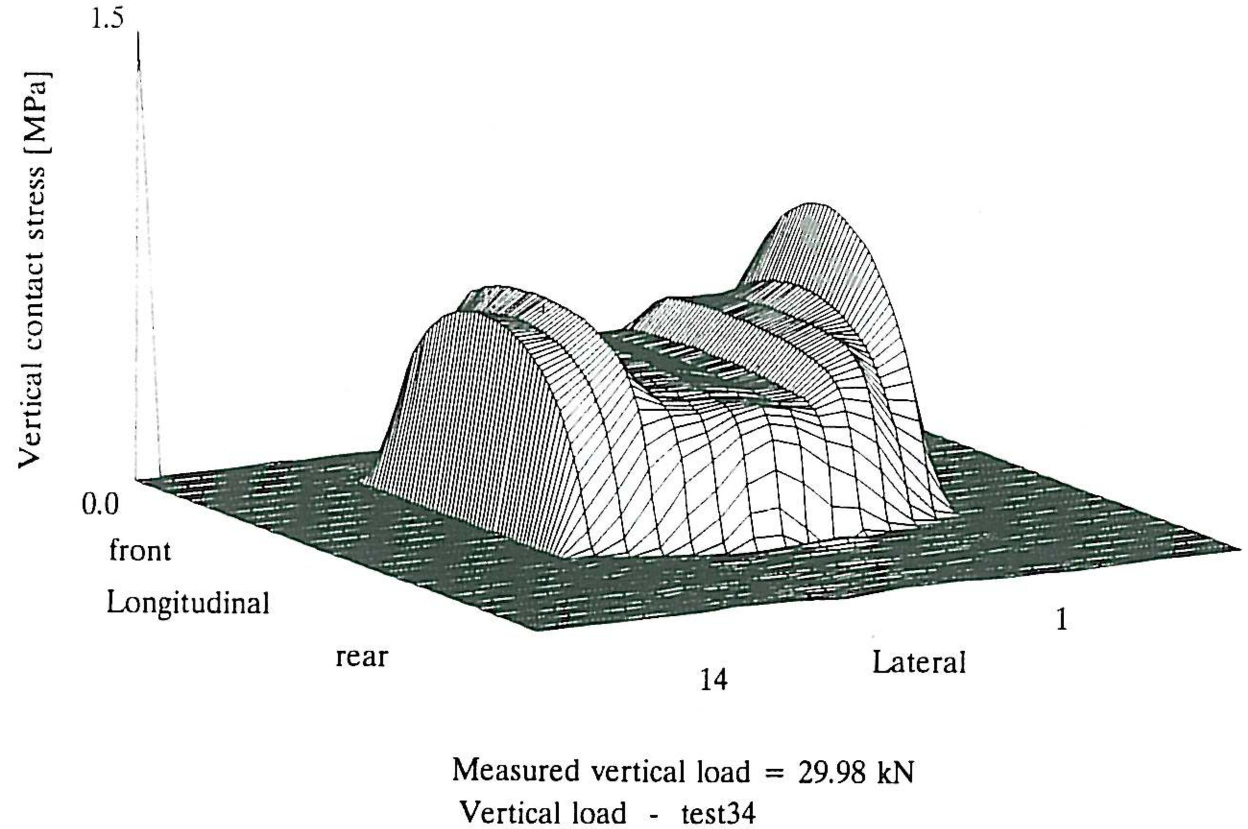

Figure 4: **Measured vertical stress distribution of a 40 kN load, tyre inflation pressure 620 kPa and a speed of 8 km/h**

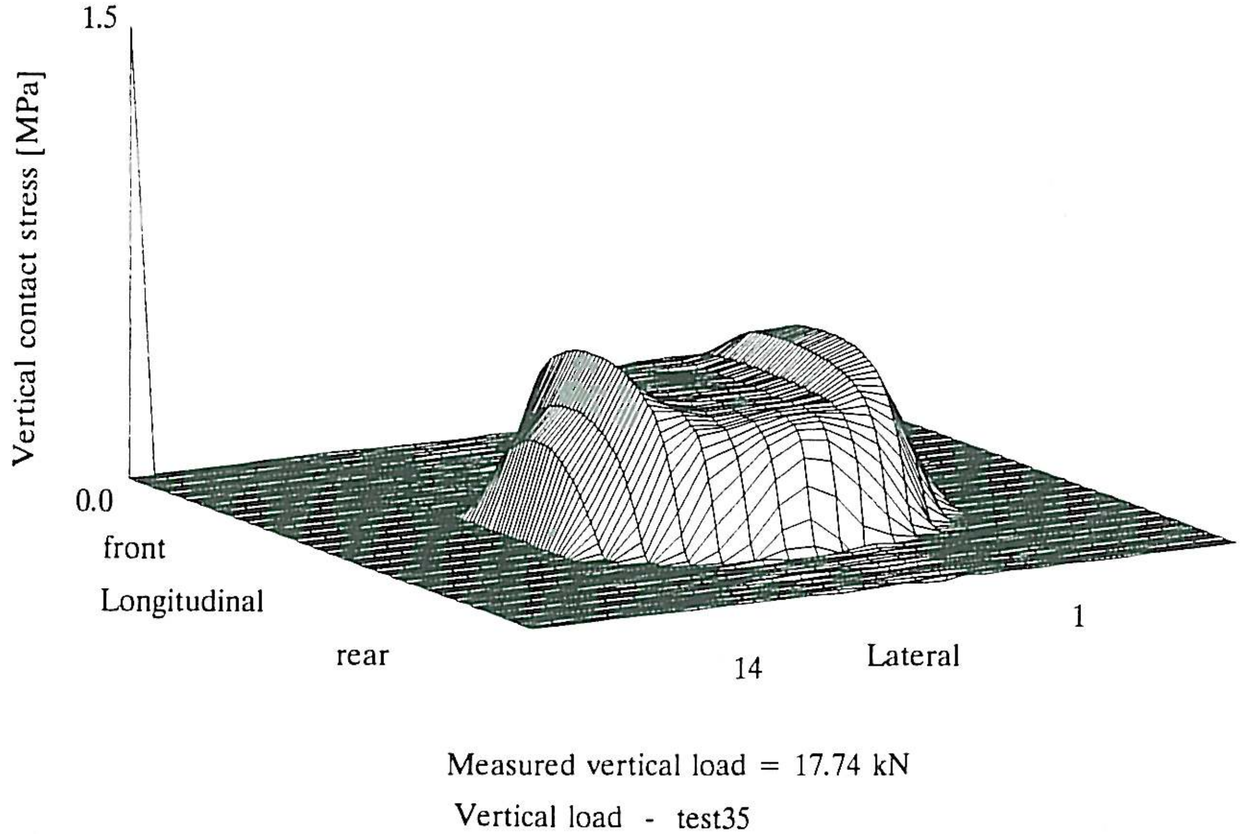

Figure 5: **Measured vertical stress distribution of a 20 kN load, tyre inflation pressure 620 kPa at a speed of 8 km/h**

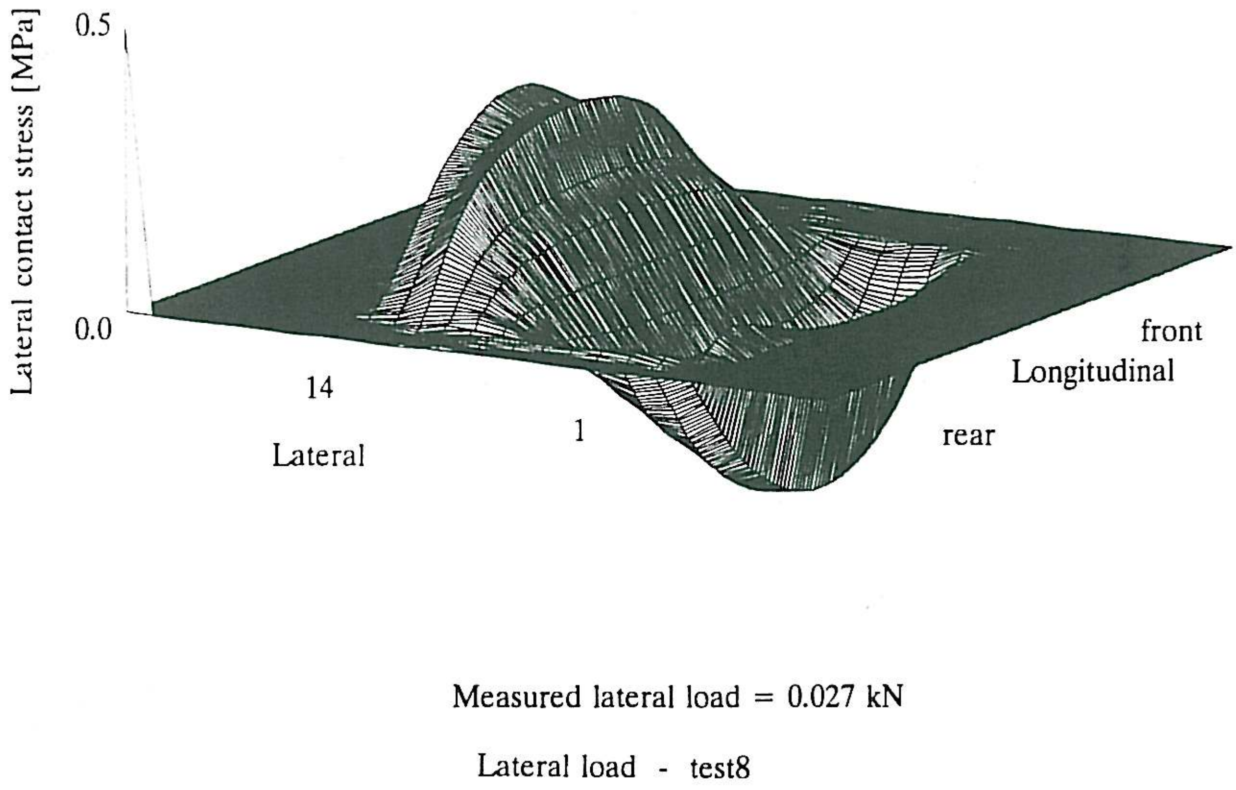

Figure 6: **Measured transverse stress distribution of a 60 kN load, tyre inflation pressure 620 kPa at a speed of 4 km/h**

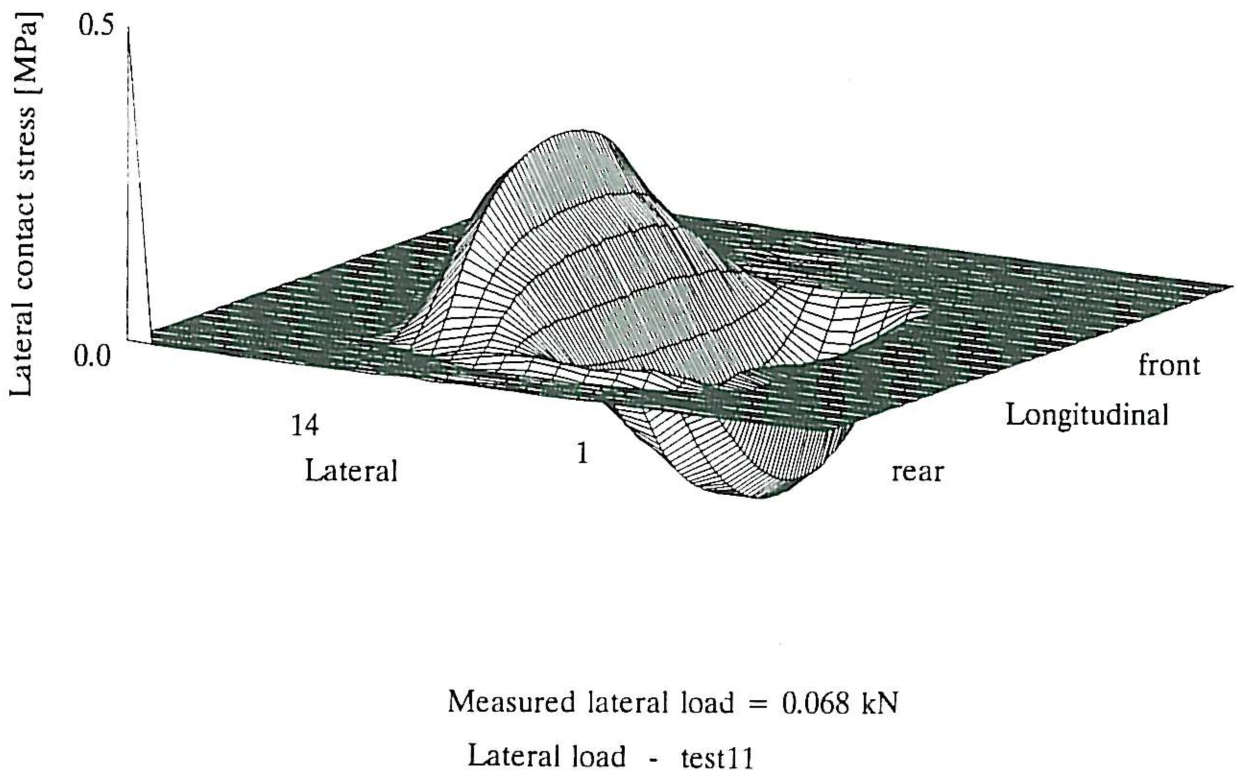

Figure 7: **Measured transverse stress distribution of a 40 kN load, tyre inflation pressure 620 kPa at a speed of 8 km/h**

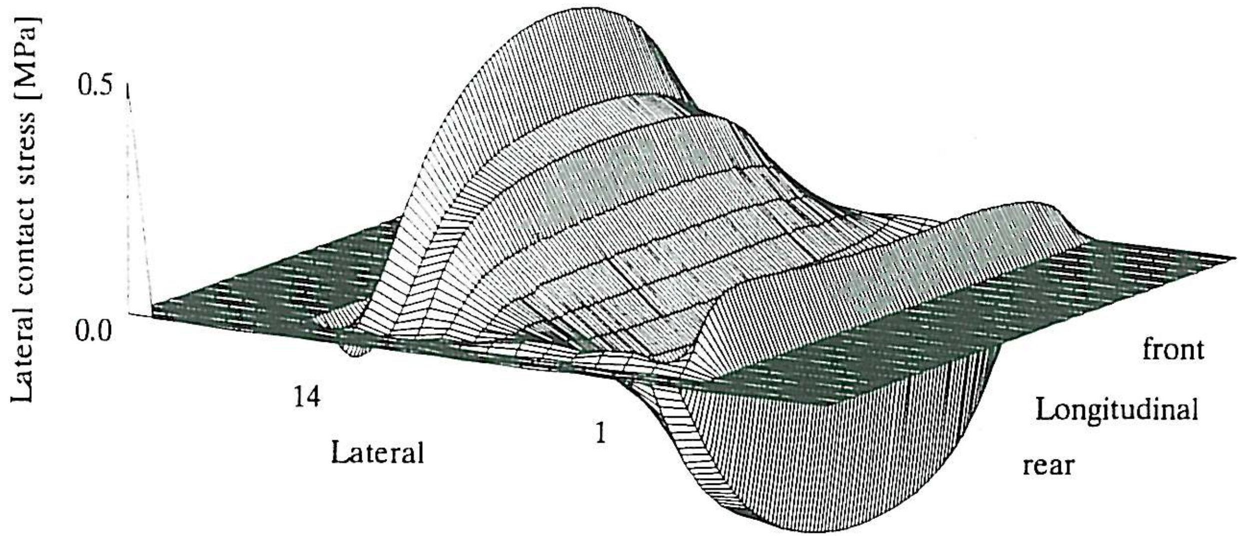

Measured lateral load = 0.747 kN

Lateral load - test17

Figure 8: **Measured transverse stress distribution of a 80 kN load, tyre inflation pressure 620 kPa at a speed of 8 km/h**

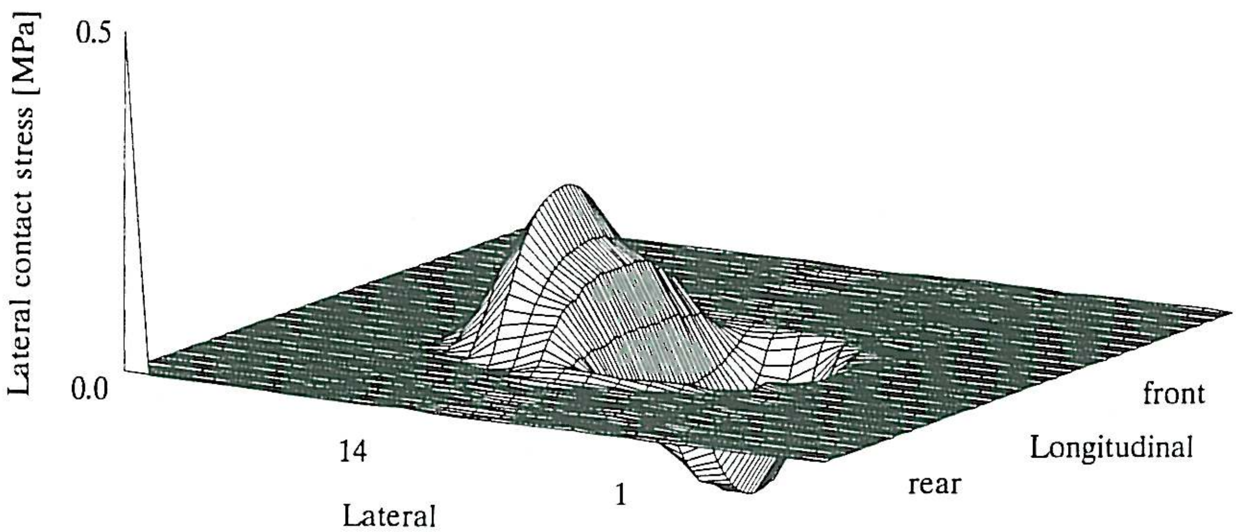

Measured lateral load = 0.016 kN

Lateral load - test28

Figure 9: **Measured transverse stress distribution of a 20 kN load (with shear), tyre inflation pressure 620 kPa at a speed of 8 km/h**

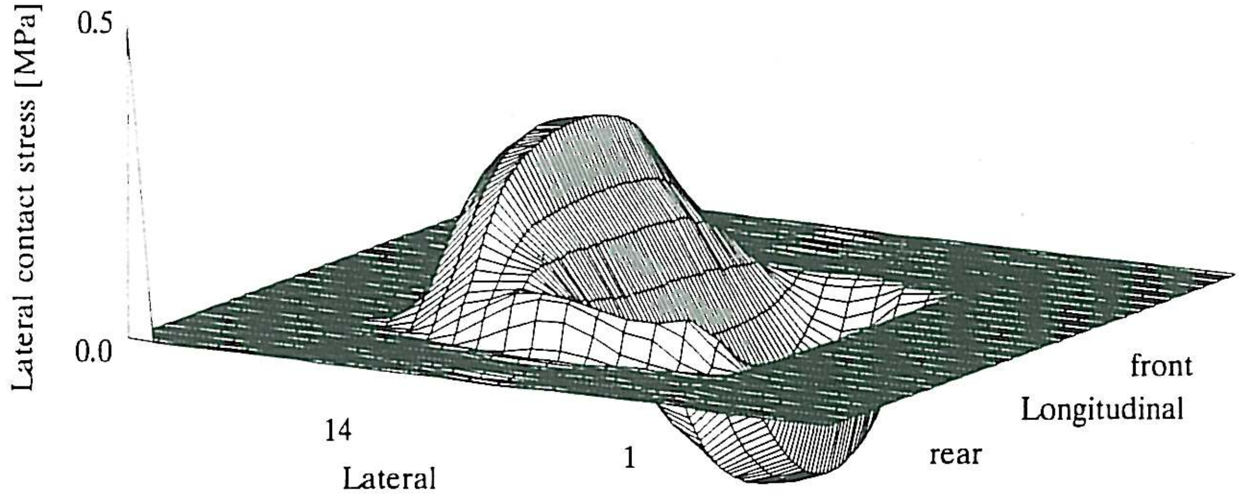

Measured lateral load = 0.814 kN
Lateral load - test29

Figure 10: **Measured transverse stress distribution of a 40 kN load (with shear), tyre inflation pressure 620 kPa at a speed of 8 km/h**

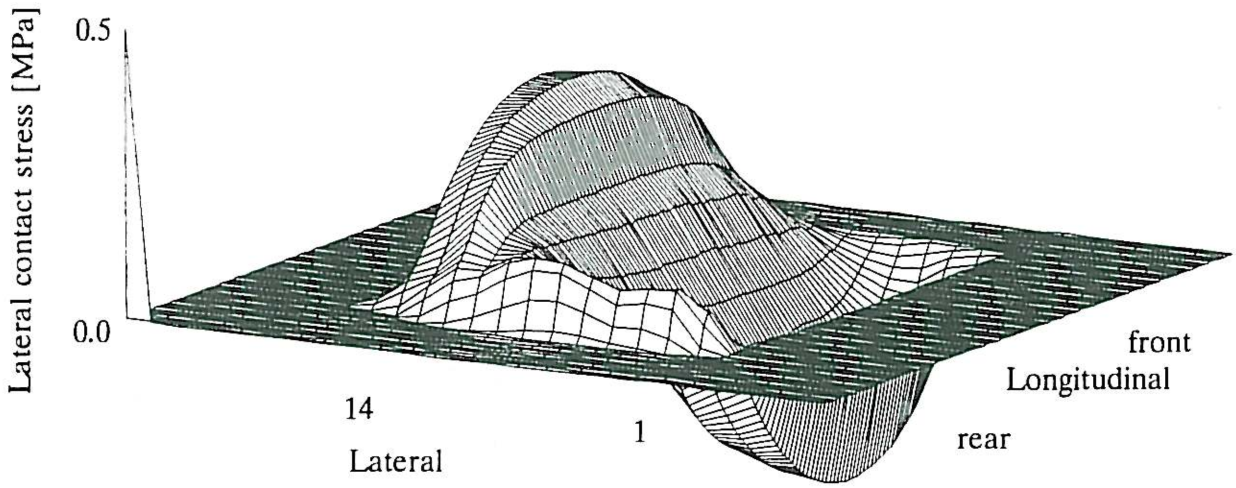

Measured lateral load = 1.24 kN
Lateral load - test30

Figure 11: **Measured transverse stress distribution of a 60 kN load (with shear), tyre inflation pressure 620 kPa at a speed of 8 km/h**

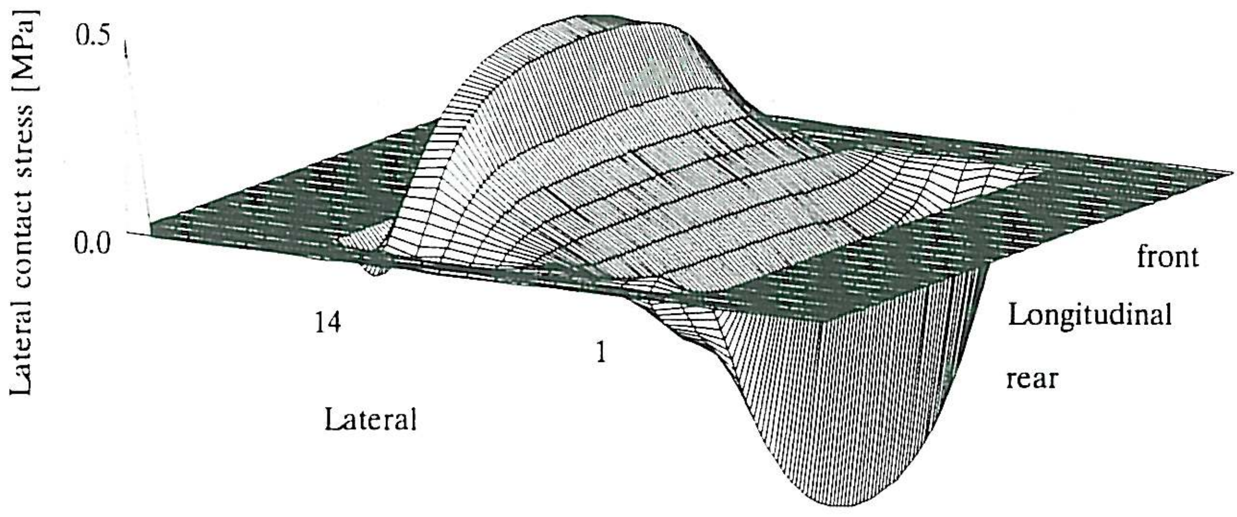

Measured lateral load = -1.416 kN
Lateral load - test31

Figure 12: **Measured transverse stress distribution of a 80 kN load (with shear), tyre inflation pressure 620 kPa at a speed of 8 km/h**

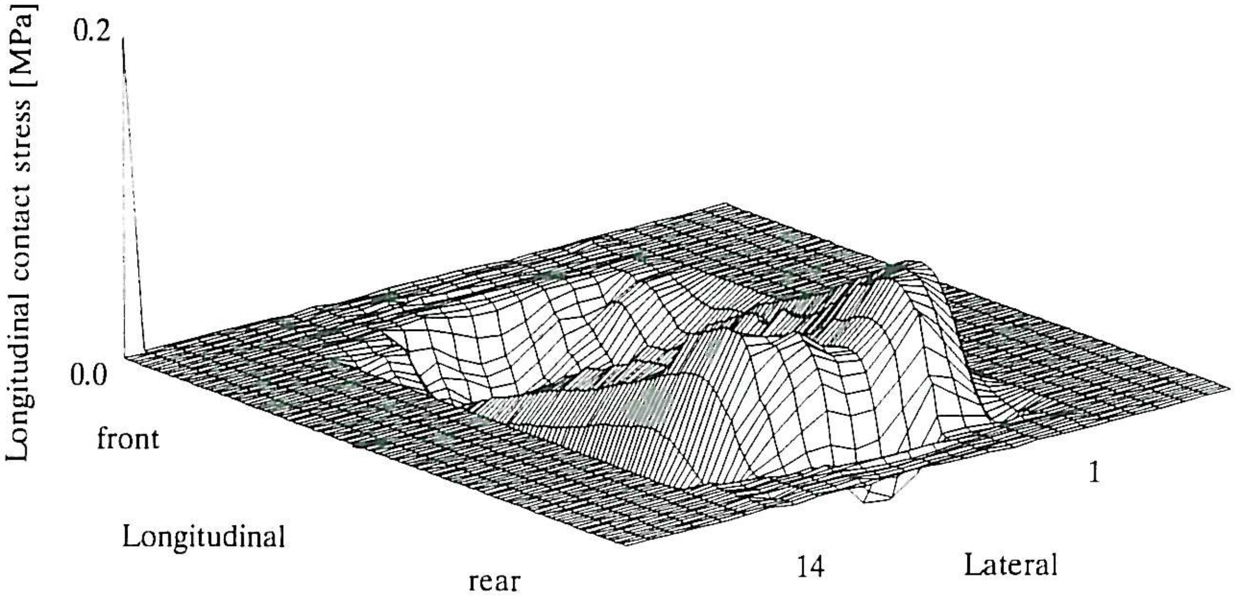

Measured longitudinal load = 0.267 kN
Longitudinal load - test3

Figure 13: **Measured longitudinal stress distribution of a 60 kN load, tyre inflation pressure 620 kPa at a speed of 8 km/h**

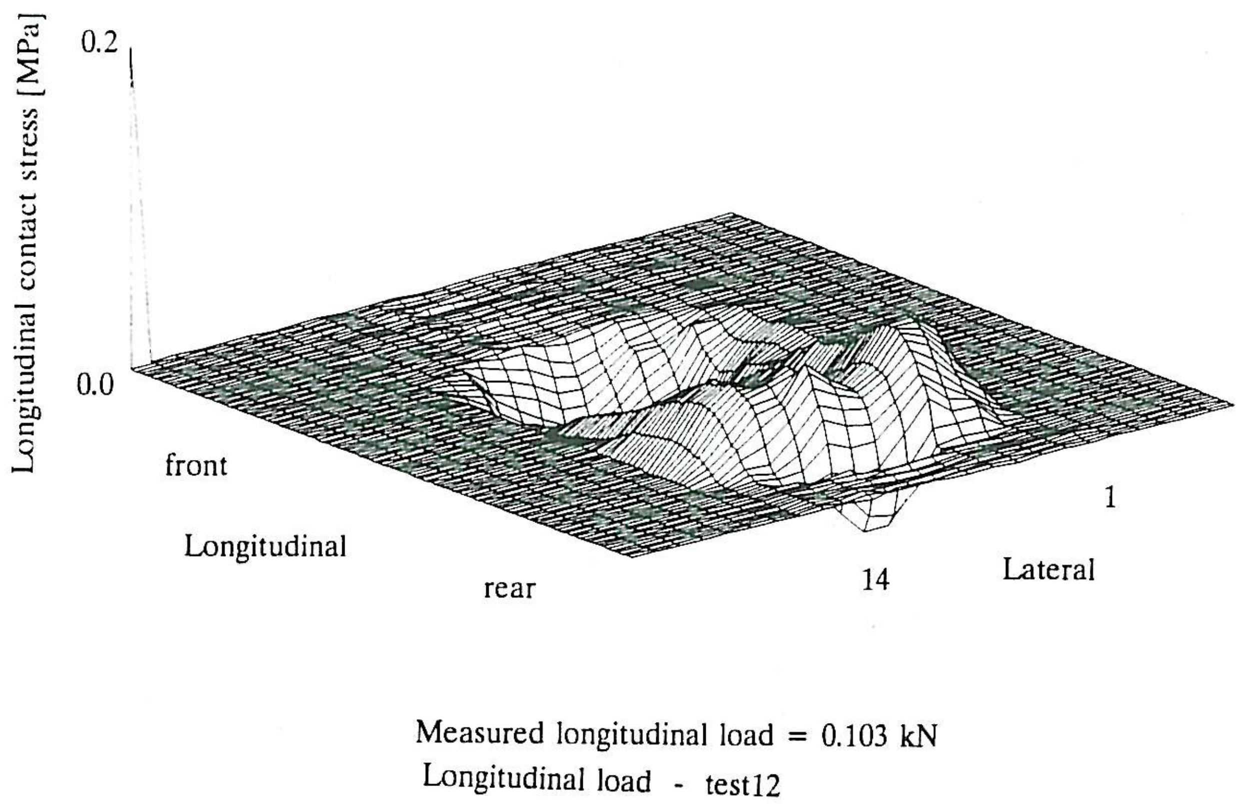

Figure 14: **Measured longitudinal stress distribution of a 40 kN load, tyre inflation pressure 620 kPa at a speed of 8 km/h**

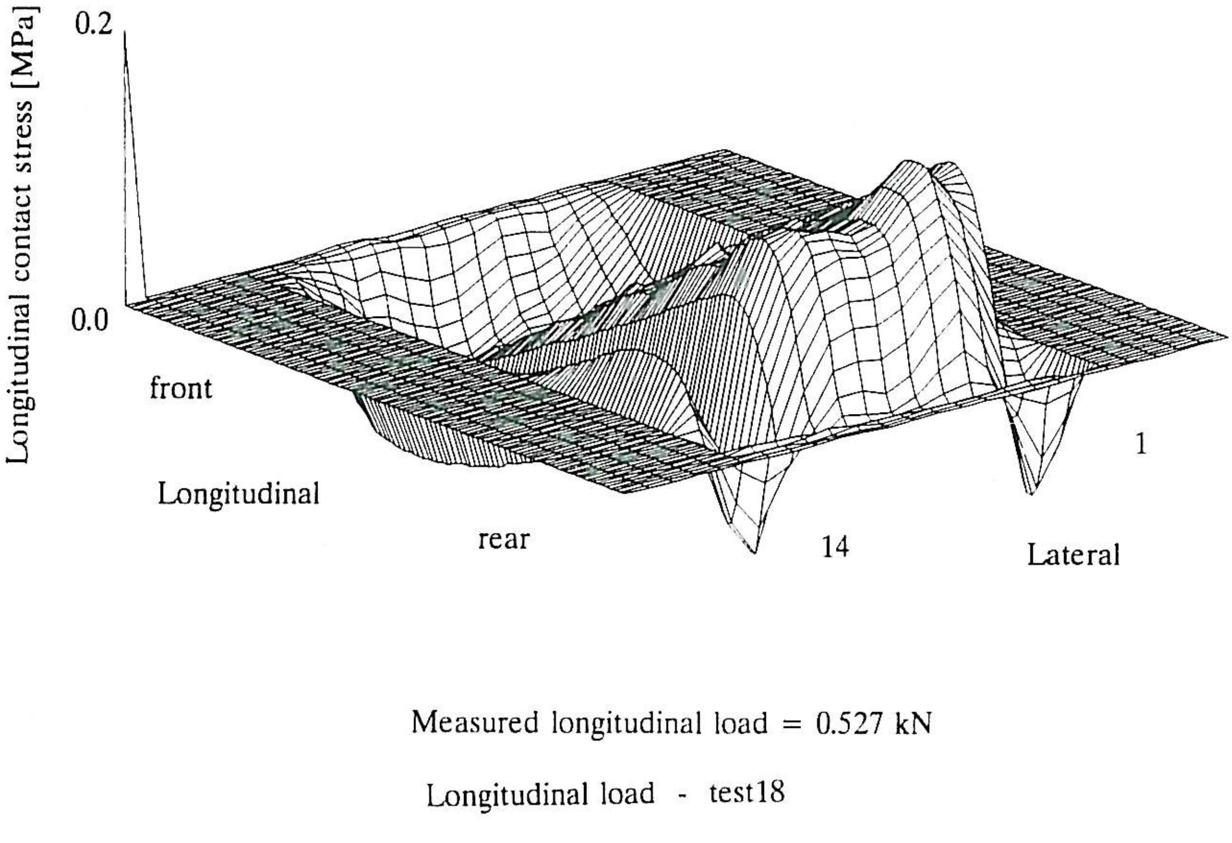

Figure 15: **Measured longitudinal stress distribution of a 80 kN load, tyre inflation pressure 620 kPa at a speed of 8 km/h**

Table 1: Test matrix and load results of the proto-type Vehicle-Road Surface Pressure Transducer Array (VRSPTA)

FIGURE NUMBER	TEST NO.	WHEEL LOAD (kN)	TYRE INFLATION PRESSURE (kPa)	VELOCITY (m/s)	DIRECTION	RESULTANT VERTICAL FORCE (kN)	RESULTANT TRANSVERSE FORCE (kN)	RESULTANT LONGITUDINAL FORCE (kN)	COMMENTS
1	1	60	620	2,222	Vertical	42,32			Varying velocity
	4	60	620	1,667	Vertical	40,34			
	7	60	620	1,111	Vertical	43,09			
2	10	40	620	2,222	Vertical	30,71			Varying wheel load
	13	60	620	2,222	Vertical	40,63			
	16	80	620	2,222	Vertical	65,56			
	19	60	620	2,222	Vertical	48,1			Varying tyre pressure
	22	60	570	2,222	Vertical	49,51			
	25	60	520	2,222	Vertical	50,83			
3	32	80	620	2,222	Vertical	52,15			Shear with varying wheel load
	33	60	620	2,222	Vertical	41,83			
4	34	40	620	2,222	Vertical	29,98			
5	35	20	620	2,222	Vertical	17,74			
	2	60	620	2,222	Transverse		0,010		Varying velocity
	5	60	620	1,667	Transverse		-0,221		
6	8	60	620	1,111	Transverse		0,027		
7	11	40	620	2,222	Transverse		0,068		Varying wheel load
	14	60	620	2,222	Transverse		-0,032		
8	17	80	620	2,222	Transverse		0,747		

Table 1: **Test matrix and load results of the proto-type Vehicle-Road Surface Pressure Transducer Array (VRSPTA) (Continued)**

FIGURE NUMBER	TEST NO	WHEEL LOAD (kN)	TYRE INFLATION PRESSURE (kPa)	VELOCITY (m/s)	DIRECTION	RESULTANT VERTICAL FORCE (kN)	RESULTANT TRANSVERSE FORCE (kN)	RESULTANT LONGITUDINAL FORCE (kN)	COMMENTS
	20	60	620	2,222	Transverse		-0,078		Varying tyre pressure shear
	23	60	570	2,222	Transverse		0,666		
	26	60	520	2,222	Transverse		0,186		
9	28	20	620	2,222	Transverse		0,016		Shear with varying wheel load
10	29	40	620	2,222	Transverse		0,814		
11	30	60	620	2,222	Transverse		1,24		
12	31	80	620	2,222	Transverse		-1,416		
13	3	60	620	2,222	Longitudinal			0,267	Varying velocity
	6	60	620	1,667	Longitudinal			0,415	
	9	60	620	1,111	Longitudinal			0,294	
14	12	40	620	2,222	Longitudinal			0,103	Varying wheel load
	15	60	620	2,222	Longitudinal			0,635	
15	18	80	620	2,222	Longitudinal			0,527	
	21	60	620	2,222	Longitudinal			0,397	Varying tyre pressure
	24	60	570	2,222	Longitudinal			0,924	
	27	60	520	2,222	Longitudinal			1,161	

8.4 Tyre/pavement interface stresses

An indication of some of the measured stresses by the VRSPTA prototype system is given in Table 2. These results indicate that tyre side wall stresses are as high as twice the tyre inflation stresses and, in addition that the maximum transverse stresses are as high as ~~27~~ 72 per cent ~~more than~~ of the inflation pressure. The maximum longitudinal stresses appear to be the lowest of the three stresses - at maximum only 30 per cent of the tyre inflation pressure. It is accepted that these stresses are possibly not exactly correct and should be viewed within the test constraints used in this particular study. The results however appear to be promising in evaluating tyre/pavement interface stress patterns with a system such as the VRSPTA used here.

Table 2: Indication of some tyre/pavement interface stresses measured by the VRSPTA

TEST NUMBER	TYPE OF STRESS	A STRESS (kPa)	B INFLATION PRESSURE (kPa)	MEASURED LOAD (kN)	RATIO A/B
1	Vertical maximum (side wall)	1 234	620	60	2
1	Vertical (centre of tyre)	798	620	60	1,15
32	Vertical maximum (side wall)	1 551	620	80	2,5
32	Vertical (centre of tyre)	788	620	80	1,27
2	Maximum transverse	444	620	60	0,72
3	Maximum longitudinal	93	620	60	0,15
6	Maximum longitudinal	102	620	60	0,17
9	Maximum longitudinal	83	620	60	0,13
18	Maximum longitudinal	178	620	60	0,29

8.5 Discussion on accuracy of the measured loads

The total vertical loads recorded by the load cell were consistently (approximately 25 per cent) lower than the HVS vertical wheel loads. Apart from the difference between the two readings, the repeatability of the measured loads was also not very high. Because of these discrepancies, it was decided to install four reference load cells underneath the base plate, and to repeat the measurements.

9. INSTALLATION OF REFERENCE LOAD CELLS

9.1 Reference load cell configuration

Because a pressure control valve was used to control the HVS vertical wheel load, there was some doubt about the accuracy and repeatability of this load which served as a reference load. Therefore it was decided to install reference load cells underneath the existing pin load cells. Four load cells were used to, amongst other, increase the stability of the load cell system.

9.2 Reference load cell details

Four 50 kN load cells were used as reference load cells. These load cells were calibrated in a 100 kN Schenck materials testing machine prior to installation. A 100 kN Schenck load cell which had been calibrated by a National Calibration Service (NCS) facility was used as the master load cell.

10. ADDITIONAL MEASUREMENTS UNDER HVS

10.1 Instrumentation and data recording equipment

The same DC strain gauge signal conditioners for the reference load cells were used for the pin load cells. The remaining equipment was identical to that used for the initial measurements. All load cells had to be re-calibrated, since the equipment had been used for other purposes since the initial measurements. Measurement procedures identical to the initial measurements were used, except that the reference load cell outputs were also recorded.

Similar results to those obtained earlier were obtained. The vertical loads obtained from the pin load cell readings were consistently lower (approximately 25 per cent) than the total reference loads indicating that the initial measurements had been correct.

11. DISCREPANCY IN TOTAL VERTICAL LOAD

The differences between the total vertical load given by the pin load cells and that given by the reference load cells may be ascribed to the geometrical differences between the instrumented conical load cell pins and the neighbouring square pins. These differences are twofold, namely the difference in top area, as well as the difference in the stiffness of the pins. The lower vertical stiffness of the instrumented pins would cause a greater deflection under load than that of the surrounding square pins. This deflection would redistribute the loads to the surrounding square pins and the load carried by the instrumented pins would be reduced, causing the total vertical load measured by the pin load cells to be less than the actual total vertical load. As mentioned in paragraph 3.3, the top area of the instrumented pins was smaller than that of the square pins, causing the instrumented pins to push deeper into the tyre rubber than the square pins. This would again redistribute the loads to the surrounding square pins and reduce the load carried by the instrumented pins.

12. RECOMMENDATIONS

One of two methods can be used to rectify the error in measured vertical load: Vertical load correction curves can be determined for a range of tyre types and pressures and the measured vertical loads can be corrected using these curves, However, some degree of uncertainty regarding the accuracy of the loads (and stresses) so obtained would always remain. The second method is to replace all the surrounding square pins with pins identical to the instrumented pins, thereby ensuring that all pins would have the same stiffness in the vertical, longitudinal and lateral directions and all pins would have identical top areas.

12.1 Improved VRSPTA system

Based on the results of the first prototype load cell, it was decided to continue development with various design improvements towards a new stand-alone VRSPTA system. The design of the new system (which was being tested and evaluated while this paper was being prepared) includes the following:

- All pins of similar geometry (shape and area).
- Simultaneous measurement and data acquisition of 20 pins in the 3 directions for wheel speeds up to 100 km/h, at a high sampling rate (200 khz per 16 channels).
- Strain gauge conditioner rack and electronic design which allows excitation voltage, Input/Output offset and amplification adjustment.
- Stand alone calibration system and procedure for all three (3) directions.
- Stand-alone data acquisition system.

It is foreseen that these design improvements would facilitate more accurate load measurements and a more user friendly data acquisition system.

13. CONCLUSIONS

- The work performed to date has proved the viability of the concept of the Vehicle-Road Surface Pressure Transducer Array (VRSPTA) for a moving single wheel load.

- The accuracy of the load cell has to be improved and proved before it can be exploited as a stand-alone product.

- Replacing the square pins with pins identical to the instrumented pins would substantially improve the accuracy of the load cell.

- A full finite element analysis of the instrumented pins as well as of the base plate would be necessary to optimise the design before load cells can be produced for the commercial market.

- An interface between the load cell and a finite element analysis package, enabling direct transfer of measured loads as nodal load inputs to a finite element mesh, would substantially enhance the useability of the VRSPTA output for pavement design purposes, especially when the pavement design is based on non-linear material properties.

14. ACKNOWLEDGEMENTS

The Laboratory for Advanced Engineering (Pty) Ltd., Centre for Structural Mechanics at the University of Pretoria is thanked for their participation and assistance in developing the VRSPTA discussed here.

The Director for the Division of Roads and Transport Technology (TRANSPORTEK) of the CSIR (Council for Scientific and Industrial Research) is also thanked for the permission to publish this work.

15. REFERENCES

1. Bonse R P H and Kuhn S H (1959). **Dynamic forces exerted by moving vehicles on a road surface.** Highway Research Board Bulletin 233, 1959.

2. Eisenmann J and Hilmer A (1987). **Influence of wheel load and inflation pressure on the rutting affect of asphalt pavements - Experiments and theoretical investigations.** Proceedings of the 6th International Conference on Structural Design of Asphalt Pavements, Volume 1, July 13 through 17, 1987, University of Michigan, Ann Arbor, Michigan, USA, pp 392-403.

3. Freeme C R, Maree J H and Walker R N (1982a). **User's simulators.** International Symposium on Bearing Capacity of Roads and Airfields, June 23 - 25, 1982, Trondheim, Norway.

4. Freeme C R, Maree J H and Viljoen A W (1982). **Mechanistic design for asphalt pavements and verification using the Heavy Vehicle Simulator.** Proceedings of the 5th International Conference on the Structural Design of Asphalt Pavements, Vol 1, Delft, Holland, August 1982, pp 156-173, CSIR Reprint RR 362.

5. Huang Yang H. **Pavement Analysis and Design.** Prentice-Hall, Inc., 1993, Englewood Cliffs, New Jersey 07632.

6. Ioannides A M, Khazanovich I (1993). **Load equivalency concepts: A mechanistic reappraisal.** Transportation Research Record (TRR) No. 1388, Transportation Research Board, National Research Council, National Academy Press, Washington, D.C., 1993.

7. Martin F (1936). **Druckverteilung in der Berührungsfläche zwischen kraftfahrzeugreifen und Fahrbahn.** Band 80, Nr 44, pp 1333-1334, 31 October 1936.

8. South African Roads Board (SARB) 1993. **Flexible pavement performance modelling under multiple wheel and axle load configurations.** Unpublished Project Report PR 92/317, Research and Development Advisory Committee (RDAC), Department of Transport, Pretoria, 1993.

9. Tielking J T and Roberts F L (1987). **Tire contact pressure and its effects on pavement strains.** A.S.C.E. Journal of Transportation Engineering, Volume 113, No. 1, 1987, pp 56-71.

10. Tielking J T and Abraham M A (1994). **Measurement of truck tire footprint pressures.** Preprint of paper presented at the 73rd Annual Meeting, Transportation Research Board, Washington D.C., January 1994.

11. Yap P (1988). **A comparative study of the effect of truck tire types on road contact pressures. Vehicle/Pavement Interaction - where the truck meets the road.** SP-765, Society of Automotive Engineers, Inc., Warrendaler, November 1988.